Synthesis and Structure Determination of a New Organically Templated Scandium Fluorophosphate Framework and Its Indium Analogue

Hyunsoo Park,*,† Ivor Bull,‡ Luming Peng,† Victor G. Young, Jr.,§ Clare P. Grey,† and John B. Parise†,‡

Department of Chemistry and Department of Geosciences, State University of New York at Stony Brook, Stony Brook, New York 11794 and Department of Chemistry, University of Minnesota, Minneapolis, Minnesota 55455

Received July 28, 2004. Revised Manuscript Received September 21, 2004

Two new isostructural scandium and indium phosphate frameworks, $(C_6H_{14}N_2)M_4F_2(PO_4)_4 \cdot 4H_2O$ (M = Sc, In), have been synthesized from hydrothermal conditions using an organic amine, 1,4-diazabicyclo[2.2.2]octane (DABCO), as a template. Their structures have been determined by single-crystal X-ray diffraction and supported by solid-state magic-angle spinning (MAS) NMR spectroscopy. They crystallize in the $P2_1/n$ space group with a = 10.283(2) Å, b = 12.698(2) Å, c = 17.864(3) Å, and β = 102.761(3)° and a = 10.280(2) Å, b = 12.700(2) Å, c = 17.860(4) Å, and β = 102.47(3)° for Sc- and In-compounds, respectively. They are built from corner-sharing M octahedra and P tetrahedra which form eight- and six-membered channels along the *b*-axis. The channels are occupied by organic templates and water molecules. All PO_4 groups share four corners with M polyhedra, resulting in a fully connected framework. The local environments around P, F, and Sc atoms in the Sc-compound were carefully examined by ^{31}P MAS, ^{19}F MAS, ^{45}Sc MAS, ^{45}Sc MQMAS, and ^{45}Sc/^{19}F REDOR NMR spectroscopy.

Introduction

Since the successful synthesis of a family of organically templated alumino-phosphates ($AlPO_4$-n) by Flanigen and co-workers,[1] a great number of metal phosphates have been induced to form open framework and layered materials.[2,3] Interests in this class of materials are driven by the need for new functionality, selective catalysis, and ion-exchange, for example, and new insights are given by exploratory synthetic and structural chemistry. The incorporation of a wider variety of species, with coordination geometries different from the corner-connected tetrahedral geometries which are traditionally associated with molecular sieves, resulted in the discovery of new structure types containing mixed tetrahedral−octahedral geometry.[3] For instance, several transition-metal phosphates such as the titanium-,[4] iron-,[5] and nickel-phosphates[6,7] have been discovered and structurally characterized.

Although a great variety of metals has been incorporated into new and known framework topologies, there are only a few reports of the successful synthesis of scandium-based open framework materials.[8−10] There are quite a few organically templated indium phosphates,[11−13] but few Sc-analogues of these materials have been investigated.[10] Recently, our group reported the synthesis of several novel three-dimensional scandium phosphate frameworks, including $(C_2N_2H_{10})_8Sc_8(ScO_2)_4(PO_4)_4(HPO_4)_{12} \cdot 12H_2O$ which contains 14- and 10-membered channels.[10] As a part of our continuing investigation on new microporous silicates and phosphates, we describe the hydrothermal syntheses and structure determinations of a scandium fluorophosphates, $(C_6N_2H_{14})Sc_4F_2(PO_4)_4 \cdot 4H_2O$ and its In-analogue $(C_6N_2H_{14})In_4F_2(PO_4)_4 \cdot 4H_2O$ using 1,4-diazabicyclo[2.2.2]-octane (DABCO) as a structure-directing agent. These materials are the first reported scandium and indium phosphate open frameworks which consist of fully connected PO_4 groups. The synthetic methods and structural characterizations of these compounds are described in this work. In addition to single-crystal X-ray diffraction, the local structure of the Sc compound was

* Author to whom correspondence should be addressed. E-mail: hyppark@notes.cc.sunysb.edu.
† Department of Chemistry, State University of New York.
‡ Department of Geosciences, State University of New York.
§ University of Minnesota.

(1) Wilson, S. T.; Lok, B. M.; Messina, C. A.; Cannan, T. R.; Flanigen, E. M. *J. Am. Chem. Soc*. **1982**, *104*, 1146−1147.
(2) Férey, G. *Chem. Mater*. **2001**, *13*, 3084−3098.
(3) Harrison, W. T. A. *Curr. Opin. Solid St. M*. **2002**, *6*, 407−413.
(4) Serre, C.; Tauelle, F.; Férey, G. *Chem. Commun*. **2003**, 2755−2765.
(5) Lii, K. H.; Huang, Y. F.; Zima V.; Huang, C. Y.; Lin, H. M., Jiang, Y. C.; Liao, F. L.; Wang, S. L. *Chem. Mater*. **1998**, *10*, 2599−2609.
(6) Guillou, N.; Gao, Q.; Forster, P. M.; Chang, J. S.; Nogues, M.; Park, S. E.; Férey, G.; Cheetham, A. K. *Angew. Chem., Int. Ed*. **2001**, *15*, 2831−2834.
(7) Chang, J. S.; Hwang, J. S.; Jhung, S. H.; Park, S. E.; Férey, G.; Cheetham, A. K. *Angew. Chem., Int. Ed.* **2004**, *43*, 2819−2822.
(8) Bull, I.; Wheatley, P. S.; Lightfoot, P.; Morris, R. E.; Sastre, E.; Wright, P. A. *Chem. Commun*. **2002**, 1180−1181.
(9) Riou, D.; Fayon, F.; Massiot, D. *Chem. Mater*. **2002**, *14*, 2416−2420.
(10) Bull, I.; Young, V.; Teat, S. J.; Peng, L.; Grey, C. P.; Parise, J. B. *Chem. Mater*. **2003**, *15*, 3818−3825.
(11) Thirumurugan, A.; Natarajan, S. *Dalton Trans*. **2003**, *17*, 3387−3391.
(12) Huang, Y. F.; Lii, K. H. *Dalton Trans*. **1998**, *24*, 4085−4086.
(13) Williams, I. D.; Yu, J. H.; Du, H. B.; Chen, J. S.; Pang, W. Q. *Chem. Mater*. **1998**, *10*, 773.

10.1021/cm048764r CCC: $27.50 © 2004 American Chemical Society
Published on Web 11/09/2004

characterized in detail by ^{31}P, ^{19}F, and ^{45}Sc magic-angle NMR spectroscopy. We also discuss the influence of various parameters such as pH and organic template on the framework geometry.

Experimental Section

Synthesis. Both compounds were synthesized under mild hydrothermal conditions using Teflon-lined 23-mL Parr autoclaves. The starting materials include scandium oxide (Sc_2O_3, 99.9%, Alfa-Aesar), indium nitrate pentahydrate ($In(NO_3)_3 \cdot 5H_2O$, 99.9%, Aldrich), phosphoric acid (H_3PO_4, 85 wt %, Alfa-Aesar), hydrofluoric acid (HF, 48 wt %, Fisher), 1,4-diazabicyclo-[2.2.2]octane (DABCO, 98%, Aldrich), and deionized water. Both products were prepared as small colorless crystals.

(a) Compound 1. In a typical synthesis of $(C_6N_2H_{14})Sc_4F_2(PO_4)_4 \cdot 4H_2O$, 1.27 g of DABCO and 0.19 g of Sc_2O_3 were first mixed with 6.00 g of deionized water. Then, 0.49 g of H_3PO_4 and 0.06 g of HF were sequentially added with stirring. The staring molar composition corresponded to 4DABCO:1Sc:1.5P:0.5F:120H_2O. The resulting gel was stirred for 2 h to ensure homogeneity and then heated at 443 K for 3 days. The pH remained slightly basic throughout the reaction, from 8.6 to 8.4. The final products were filtered, washed with deionized water, and dried in air. They consisted of small hexagon-shaped crystals and a small amount of amorphous powders. The suitable crystals were picked from the matrix for single-crystal X-ray diffraction, TGA, and NMR spectroscopy.

(b) Compound 2. In a typical synthesis of $(C_6N_2H_{14})In_4F_2(PO_4)_4 \cdot 4H_2O$, 0.26 g of DABCO and 0.54 g of $In(NO_3)_3 \cdot 5H_2O$ were first dissolved in 3.84 g of deionized H_2O. Then, 0.26 g of H_3PO_4 and 0.06 g of HF were added with stirring. The starting molar ratios were thus 5DABCO:3In:5P:3F:478H_2O. After being stirred for 2 h, the reactant gel was heated at 463 K for 3 days. The resulting products were rhombus-shaped crystals and a small amount of amorphous powders. The pH of the reaction changed from 7.0 to 8.2.

Initial Characterization. Phase purity and crystallinity were determined by powder X-ray diffraction method using a Scintag diffractometer with CuKα radiation (step size of 0.02° and counting time of 1.2 s/step) in a 2θ range of 3−50°. The XRD patterns of both compounds are given in Figure 1. The patterns are consistent with the structures determined by single-crystal X-ray diffraction.

Crystal Structure Determination. A suitable single crystal from each compound was selected under polarizing microscope and was attached to the tip of a glass fiber. The raw intensity data were integrated using the software SAINT,[14] and an empirical absorption correction was applied using SADABS.[15] The crystal structures were solved via direct method using SHELXS[16] and refined anisotropically with SHELXL.[16] The details of the structure determinations are given in Table 1.

(a) Compound 1. Data collection and structure determinations were carried out on a Bruker P4 diffractometer equipped with a CCD detector at the Department of Chemistry, University of Minnesota. The data were collected at 173 K with MoKα radiation with an exposure time of 30 s per frame and a detector distance of 4.0 cm. A randomly oriented region of reciprocal spaces was examined to a resolution of 0.77 Å. Four major sections of frames were collected with a step size of 0.30° in ω at four different ϕ settings. The final unit cell constants were determined from 2021 strong reflections after integration.

(b) Compound 2. Data collection was performed on an in-house Bruker P4 diffractometer with a SMART CCD detector. The data were collected at room temperature with an exposure time of 30 s per frame with a detector distance of 5.016 cm. Five sections of frames were collected with a step width of 0.30° in ϕ. The unit cell parameters were calculated and refined from all the intensities $I > 15\sigma(I)$.

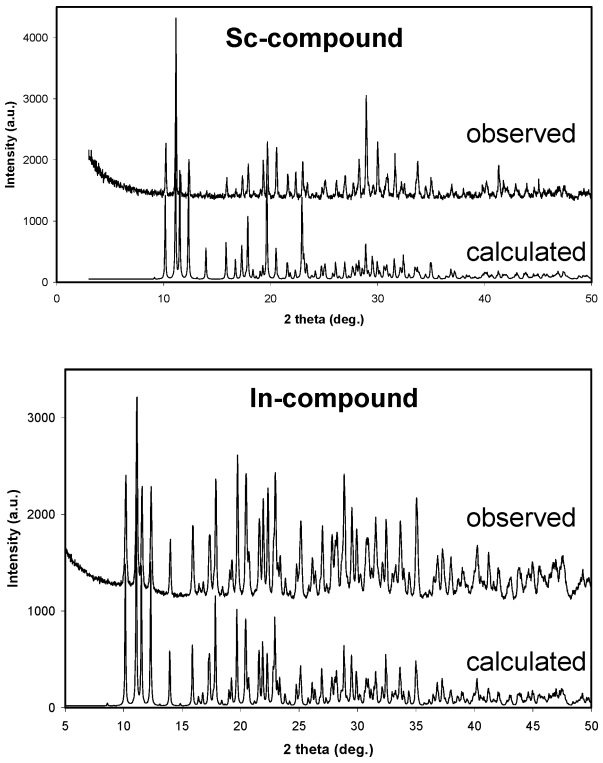

Figure 1. Powder X-ray diffraction patterns of $(C_6H_{14}N_2)Sc_4F_2(PO_4)_4 \cdot 4H_2O$ (above) and $(C_6H_{14}N_2)In_4F_2(PO_4)_4 \cdot 4H_2O$ (below).

Thermal Analysis of Compound 1. Thermogravimetric analysis-differential scanning calorimetry (TGA/DSC) was performed on a Netzsch STA 449C instrument with a heating rate of 5.0 °C/min. The TG curve in Figure 2 displays the events between 30 and 750 °C. It shows that water molecules are lost before 120° (9.1%; theoretical: 9.2%). Organic molecules are removed progressively between 160 and 320 °C (weight loss: 17.8%; theoretical: 16.0%). The absence of the peaks from the powder X-ray diffraction of the resulting materials indicates that the framework collapses quickly upon the removal of the organic amines.

Solid-State NMR Spectroscopy of Compound 1. ^{31}P, ^{1}H-decoupled, MAS NMR experiments were carried out using a double-tuned Chemagnetics 4.0 mm probe on a Chemagnetics CMX-360 spectrometer at Larmor frequencies of 145.7 MHz (^{31}P) and 360.13 MHz (^{1}H). ^{19}F and ^{45}Sc MAS NMR experiments were performed with a double-tuned Bruker 2.5-mm probe on a Bruker AVANCE 600 spectrometer at Larmor frequencies of 145.8 and 564.7 MHz, respectively. A rotor-synchronized Hahn echo ($\pi/2 - \tau - \pi - \tau -$ acquire; $\tau = 1$ rotor period) was used to acquire the one-dimensional ^{19}F MAS spectra. The ^{19}F two-dimensional (2D) double quantum (DQ) MAS NMR spectra were obtained with a BABA (back-to-back) dipolar recoupling sequence.[17] A single-pulse sequence with a flip angle of $\pi/8$ was used to acquire MAS spectra from the $I = 5/2$ (100% abundant) nucleus ^{45}Sc. 2D ^{45}Sc triple-quantum MAS (3QMAS) NMR spectrum was obtained using a three-pulse z-filter sequence.[18] t_1 increments of one rotor period were used for both the 2D DQ and 3QMAS experiment. $^{45}Sc/^{19}F$ REDOR experiments used standard REDOR sequences[19]

(14) *SAINT V6.2*; Bruker Analytical X-ray Systems: Madison, WI, 2002.

(15) Sheldrick, G. M. *SADABS*, a program for the Siemens Area Detector Absorption Program; Bruker-AXS: Madison, WI, 2001.

(16) Sheldrick, G. M. *SHELXL,* V.6.10; Bruker-AXS: Madison, WI, 2000.

(17) Feike, M.; Demco, D. E.; Graf, R.; Gottwald, J.; Hafner, S.; Spiess, H. W. *J. Magn. Reson., Ser. A* **1996**, *122*, 214−221.

(18) Amoureux, J. P.; Fernandez, C.; Steuernagel, S. *J. Magn. Reson., Ser. A* **1996**, *123*, 116−118.

(19) Pan, Y.; Gullion, T.; Schaefer, J. *J. Magn. Reson.* **1990**, *90*, 330−340.

Table 1. Crystallographic Data of $(C_6H_{14}N_2)M_4F_4(PO_4)_4{\cdot}4H_2O$

empirical formula	$C_6H_{22}F_2N_2O_{20}P_4Sc_4$	$C_6H_{22}F_2N_2O_{20}P_4In_4$
formula weight	783.98	1063.41
collection temperature	173(2) K	298(2) K
wavelength	0.71073 Å	0.71073 Å
space group	$P2_1/n$	$P2_1/n$
unit cell dimensions	$a = 10.283(2)$ Å	$a = 10.280(2)$ Å
	$b = 12.698(2)$ Å	$b = 12.700(3)$ Å
	$c = 17.864(3)$ Å	$c = 17.860(4)$ Å
	$\beta = 102.761(3)°$	$\beta = 102.47(3)°$
volume	2274.8(6) Å^3	2276.7(8) Å^3
Z, calculated density	4, 2.289 g/cm^3	4, 3.102 g/cm^3
absorption coefficient	1.539 mm^{-1}	4.40 mm^{-1}
F(000)	1576	2024
crystal size	0.15 mm × 0.08 mm × 0.04 mm	0.20 mm × 0.10 mm × 0.08 mm
θ range for data collection	1.98−27.52°	1.98−28.31°
index ranges	$-13 \le h \le 13$	$-13 \le h \le 13$
	$0 \le k \le 16$	$-15 \le k \le 16$
	$0 \le l \le 23$	$-23 \le l \le 22$
total reflections	22791	16644
independent reflections	5236 [R(int) = 0.0832]	5309 [R(int) = 0.0599]
completeness to θ	99.8%	93.6%
absorption correction	SADABS	SADABS
max and min transmission	0.9410 and 0.8019	0.703 and 0.522
refinement method	full-matrix least squares on F^2	full-matrix least squares on F^2
data/restraints/parameters	5236/289/428	5309/0/358
goodness-of-fit	1.061	0.994
final R [$I > 2\sigma$(I)]	$R1 = 0.0418$, w$R2 = 0.0984$	$R = 0.0395$, w$R2 = 0.0897$
R (all data)	$R1 = 0.0604$, w$R2 = 0.1068$	$R1 = 0.0574$, w$R2 = 0.0977$
largest difference peak and hole	0.709 and −0.554 eÅ^{-3}	1.45 and −1.24 eÅ^{-3}

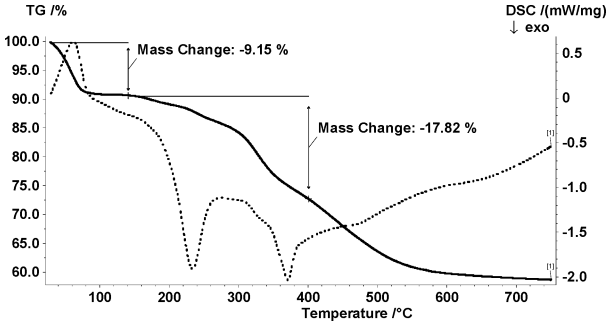

Figure 2. TGA/DSC curve of $(C_6H_{14}N_2)Sc_4F_2(PO_4)_4{\cdot}4H_2O$ in air (heating rate = 5.0 °C/min)

chosen so as to avoid applying a string of π pulses to the quadrupolar nucleus (^{45}Sc). The pulse sequences and the coherence pathways of 2D DQ MAS NMR, 3QMAS NMR, and pulse sequences of REDOR NMR are given as supplemental information (see Supplementary Figure 1). All recycle delays were optimized experimentally. The reported chemical shifts were referenced to external standard, 85% H_3PO_4 solution, hexafluorobenzene (C_6F_6) and 0.1 mol·L^{-1} $ScCl_3$ solution, for ^{31}P, ^{19}F, and ^{45}Sc, which were set at 0, −163, and 0 ppm, respectively. The ^{31}P and ^{19}F chemical shift anisotropy (CSA) simulations were done with the WSolids NMR simulation package developed by Dr. K. Eichele. The CSA convention used in this study was introduced by Haeberlen.[20]

Results and Discussion

Structural Description. The crystal structure of these compounds is depicted in Figures 3 and 4. Both $(C_6N_2H_{14})Sc_4F_2(PO_4)_4{\cdot}4H_2O$ (compound **1**) and $(C_6N_2H_{14})$-$In_4F_2(PO_4)_4{\cdot}4H_2O$ (compound **2**) contain the same new three-dimensional mixed octahedral−tetrahedral framework. Two crystallographic locations of fluorine atoms in the unit cell were deduced from the examination of the thermal parameters during the structure refinement

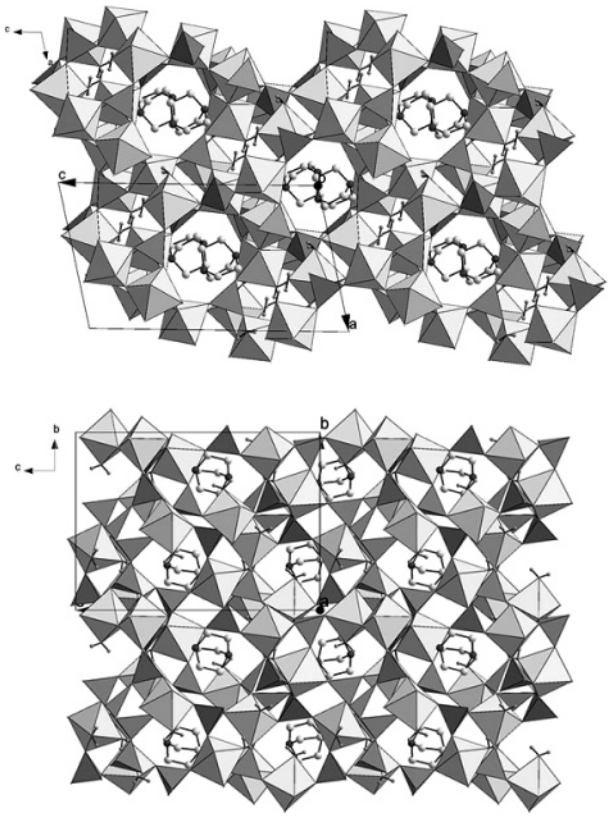

Figure 3. Crystal structure of $(C_6H_{14}N_2)M_4F_2(PO_4)_4{\cdot}4H_2O$ viewed along the *b*-axis (above) and the *a*-axis (below). DABCO molecules occupy the eight-membered rings composed of M octahedra and P tetrahedra.

and later confirmed by ^{19}F solid-state MAS NMR spectroscopy. This framework is formed by corner-sharing $MO_4F(OH_2)$, $MO_4(OH_2)_2$, and MO_4F_2 octahedra and PO_4 tetrahedra. The Sc−O bond lengths range from 2.01 to 2.13 Å and they agree with the previously reported values in scandium phosphates.[9,10] The Sc−F

(20) Haeberlen, U. *Advances in Magnetic Resonance,* Suppl. 1; Waugh, J. S., Ed.; Academic Press: New York, 1976.

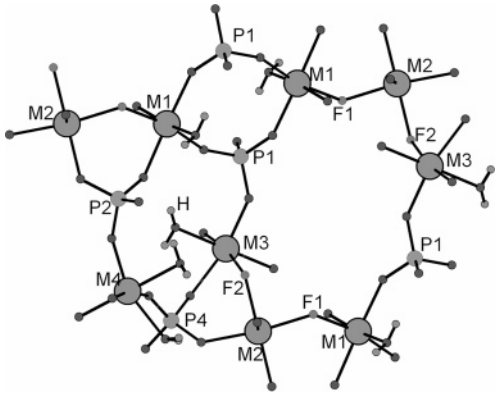

Figure 4. Details of the inorganic framework of $(C_6H_{14}N_2)$-$M_4F_2(PO_4)_4 \cdot 4H_2O$ viewed near (010) direction. It consists of four-, six-, and eight-membered rings. The amine molecules were omitted for clarity. Water molecules point away from the eight-membered rings to occupy the six-membered channels. In the eight-membered ring, M octahedra are linked via F−M−F bridges.

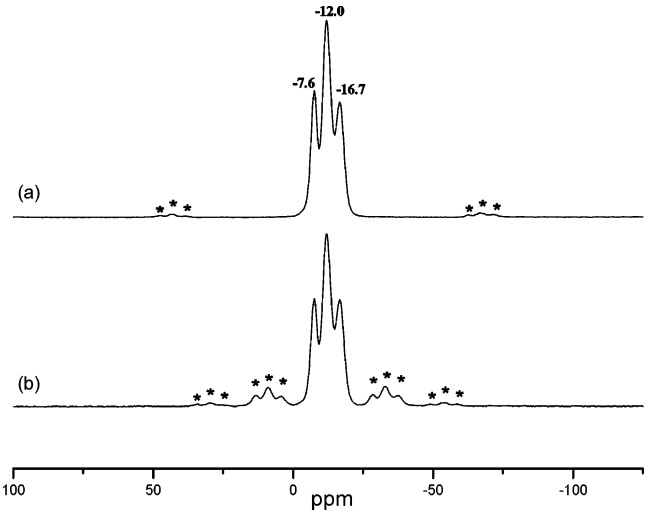

Figure 5. ^{31}P one-pulse MAS NMR spectra of compound **1**. Spinning speed: (a) 8 kHz (b) 3 kHz. Recycle delay: 15 s. Asterisks denote spinning sidebands.

bond lengths are similar to those of the Sc−O bonds, ranging from 2.05 to 2.08 Å. The In−O and In−F bond lengths are slightly larger than their Sc counterparts, varying from 2.07 to 2.16 Å and 2.11 to 2.12 Å, respectively. However, the M−OH_2 bonds are considerably longer, as they range from 2.18 to 2.26 Å. As a result, all the M atoms (except M(2) which is not bonded to water) lie in somewhat distorted octahedral environments, as also seen by the bond angles around M. The distortions in the Sc coordination environments in the Sc-compound were further examined with ^{45}Sc multiple quantum NMR spectroscopy.

The P−O bond distances vary from 1.52 to 1.56 Å in both compounds, which are in a typical range for tetrahedral P coordination. Interestingly, there are no terminal dangling P−O bonds in the framework since each PO_4 tetrahedron shares all four corners with the Sc atoms. All the previously reported scandium and indium phosphate open frameworks are built from the incomplete frameworks with dangling P−OH bonds. The formation of the complete framework without any terminal P−O bonds may be attributed to the mildly basic or neutral nature of the reaction mixtures (pH = 8.6 and 7.0 for compounds **1** and **2**, respectively) which suppresses the protonation of oxygen atoms. It is also possible that fluoride ions may catalyze the formation of M−O−P linkages at this pH range, as seen in the formation of Si−O−Si bridges in pure silica ITQ-4.[21]

The inorganic framework carries negative charges, which are balanced by the presence of the diprotonated amine molecules. There is strong hydrogen bonding present between the protons from the amino group and the fluorine atoms from the framework with the N(2)···H···F(2) distances of 2.99 Å and 3.18 Å for compounds **1** and **2**, respectively. The framework is made up of six- and eight-membered rings along the *b*-axis as well as additional six-membered rings along the *a*-axis (Figure 4). The eight-membered rings are composed of six M octahedra and two P tetrahedra. Two neighboring six- and eight-membered channels are linked via M(1)−F(1)−M(2) bridges, and they share M(3) and P(2) polyhedra. These F−metal−F bridges are often observed in gallium[22−25] and indium fluorophosphates.[11,12]

Compound **1** is the first scandium phosphate whose framework incorporates fluorine atoms. In the previously known Sc-phosphates,[9,10] fluoride ions strictly behave as a mineralizer since they do not participate in the formation of the frameworks. In the syntheses of compounds **1** and **2**, the addition of HF was essential to the formation of the desired crystals. Without HF, only dense-phase $Sc_4(PO_4)_4 \cdot 8H_2O$[10] was obtained as crystalline products in the Sc-compound preparation. Only amorphous powders were recovered in the In-compound.

The organic templates, which are located in the eight-membered channels, are disordered in both compounds. As seen in Figure 4, the six-membered rings are occupied by water molecules which are bonded to M atoms. Water molecules point toward the six-membered channels, leaving the eight-membered rings effectively dry. As a result, there are no significant hydrogen-bonding interactions present between the water molecules and the organic amines.

Solid-State NMR Results. ^{31}P MAS NMR (Figure 5) of Compound **1** shows three overlapping resonances at −7.6, −12.0, and −16.7 ppm, with relative intensities, obtained by deconvolution, of approximately 1:2:1, which corresponds to the four crystallographic distinct phosphorus sites. The resonance at −12.0 ppm is due to two of the phosphorus sites, which cannot be resolved by simple one-pulse NMR. The P−O bond lengths of P1 and P2 sites are very similar to each other, but somewhat different from those of P3 and P4 sites (1.53−1.54 Å for P1and P2 vs 1.52−1.55 Å for P3 and P4) and so the resonance at −12.0 ppm can be tentatively assigned to P1 and P2 sites. The ^{31}P chemical shift anisotropies, CSAs (Table 2), were determined by simulation of the spectrum obtained at a spinning speed

(21) Barrett, P. A.; Camblor, M. A.; Corma, A.; Jones, R. H.; Villaescusa, L. A. *J. Phys. Chem. B* **1998**, *102*, 4147−4155.
(22) Estermann, M.; McCusker, L. B.; Baerlocher, C.; Merrouche, A.; Kessler, H. *Nature* **1991**, *352*, 320.
(23) Loiseau, T.; Férey, G. *J. Mater. Chem*. **1996**, *6*, 1073−1074.
(24) Beitone, L.; Marrot, J.; Loiseau, T.; Férey, G. *Microporous Mesoporous Mater.* **2002**, *56*, 163−174.
(25) Beitone, L.; Marrot, J.; Loiseau, T.; Férey, G.; Henry, M.; Huguenard, C.; Gansmuller, A.; Taulelle, F. *J. Am. Chem. Soc*. **2003**, *125*, 1912−1922.

Table 2. ^{31}P Chemical Shift Parameter of Compound 1

δ_{iso}/ppm	$\Delta\sigma$/ppm	η
−7.6	33	0.90
− 12.0[a]	33[a]	0.9−1.0[a]
− 15.3	32	0.90

[a] Since this number results from the simulation of a line shape with equal contributions from two sites (P1 and P2), the values for $\Delta\sigma$ and in particular η are subject to some error. Since the values of $\Delta\sigma$ are so small, no attempt to model the data by using two different CSA tensors was made. Nonetheless, the qualities of the fits suggested similar values for the CSA paramaters for both sites.

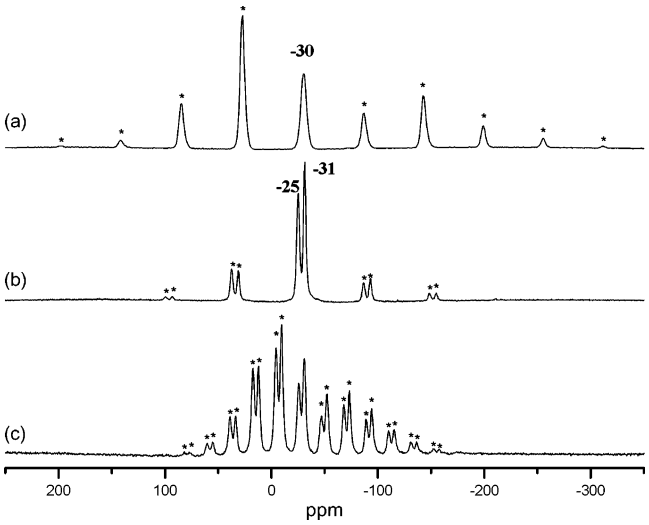

Figure 6. ^{19}F Hahn echo MAS NMR spectra of ScF_3 (a) at a spinning speed of 32 kHz and compound **1** at a spinning speed of (b) 35 kHz and (c) 12 kHz. Recycle delay: 7 s. Asterisks denote spinning sidebands.

Table 3. ^{19}F Chemical Shift Parameter of Compound 1 and ScF_3

F site	δ_{iso}/ppm	$\Delta\sigma$/ppm	η
F1 in compound **1**	−25	−150	0.55
F2 in compound **1**	−31	−140	0.60
F in ScF3	−30	−310	0.20

of 3 kHz. The $\Delta\sigma$ and η values are typical for PO_4 groups.[26,27]

^{19}F Hahn echo MAS NMR spectra (Figure 6) show two well-resolved resonances, consistent with the two Sc−F−Sc sites found by diffraction. The ^{19}F chemical shifts of the two resonances (−25 and −31 ppm) are close to that of the model compound ScF_3 (−30 ppm) which contains corner-sharing ScF_6 octahedra (Figure 6a). The ^{19}F CSAs of compound **1** and ScF_3 (Table 3) were determined from the spectra obtained at spinning speeds of 12 kHz and 32 kHz, respectively. The CSAs are much larger than any other anisotropic interactions. For example, the largest homonuclear ^{19}F dipolar coupling corresponding to that between F1 and F2 (see below) is only 4.7 kHz, corresponding to only 8.4 ppm for ^{19}F at a field strength of 14.1 T. Thus, while this interaction will result in significant contributions to the ^{19}F line shapes in ^{19}F 1D spectrum at low fields, it is not the dominant contribution at high fields. Our neglect

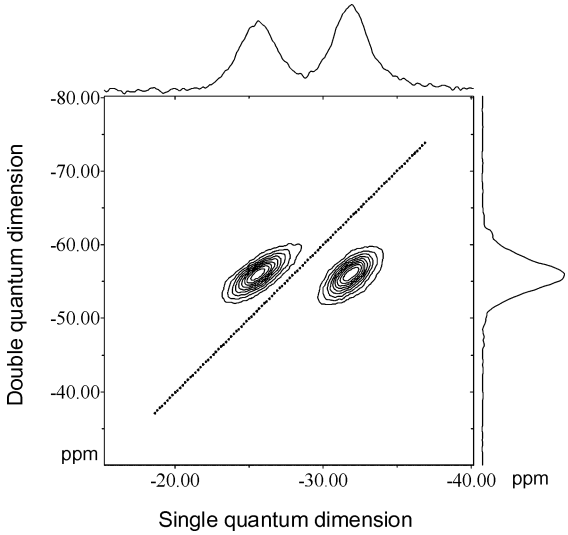

Figure 7. ^{19}F 2D double quantum MAS NMR spectra of compound **1**. Spinning speed: 35 kHz. The optimized double quantum excitation time was 0.114 ms. Recycle delay: 7 s.

of the dipolar coupling when estimating $\Delta\delta$ and η clearly introduces errors into their determination (of approximately 6% for $\Delta\delta$, on the basis of the size of the ^{19}F dipolar coupling), but they are not large that the measured CSA values cannot be used to infer structural information. There is only one scandium site in ScF_3, which adopts a distorted ReO_3 structure with Sc−F−Sc bond angles of 175.79°.[28] The nearly linear Sc−F−Sc connectivity is consistent with the very small value of η obtained for this compound of about 0.2, which is a measure of the distortion of the ^{19}F environment from axial symmetry. According to the crystallographic data, much smaller bond angles of 131.21° (Sc1−F1−Sc2) and 125.79° (Sc2−F2−Sc3) are present in compound **1**. We tentatively assign the resonance at −25 ppm, which has a smaller value of η, to the F1 site, which has the larger Sc−F−Sc bond angle, and resonance at −31 ppm to the F2 site.

On the basis of the structural refinements, the F1 and F2 sites are located in close proximity to each other, pairs of F1 and F2 ions being located at an F1−F2 distance of 2.82 Å (Figure 4). In contrast, two fluorine atoms on the same crystallographic sites (i.e., the F1−F1 and F2−F2 distances) are more than 6 Å apart. These predictions made by diffraction may be readily tested by 2D DQ MAS NMR, which represents a method for measuring homonuclear (^{19}F−^{19}F) dipolar coupling and thus the spatial proximity between sites. Characteristic resonances are observed in the 2D DQ spectrum for a material containing two sites (1 and 2) with NMR frequencies ω_1 and ω_2. If the two sites are close together, two peaks are seen at (ω_1, $\omega_1 + \omega_2$) and (ω_2, $\omega_1 + \omega_2$), where ω_A and ω_B for a peak at (ω_A, ω_B) correspond to the frequencies in the single and double quantum dimensions, respectively. In contrast, when site 1 is near a second site 1, and site 2 is near 2 only, a different set of peaks is seen at (ω_1, $2\omega_1$) and (ω_2, $2\omega_2$). The ^{19}F 2D DQ MAS NMR of compound 1 (Figure 7) only contains resonances (ω_A, ω_B) at (−25, −56) and (−31, −56). Since ω_B corresponds to the sum of the frequencies of the F1

(26) Rothwell, W. P.; Waugh, J. S.; Yesinowski, J. P. *J. Am. Chem. Soc.* **1980**, *102*, 2637−2643.
(27) Jakeman, R. J. B.; Cheetham, A. K. *J. Am. Chem. Soc.* **1988**, *110*, 1140−1143.
(28) Losch, R.; Hebecker, C.; Ranft, Z. *Z. Anorg. Allg. Chem.* **1982**, *491*, 199−202.

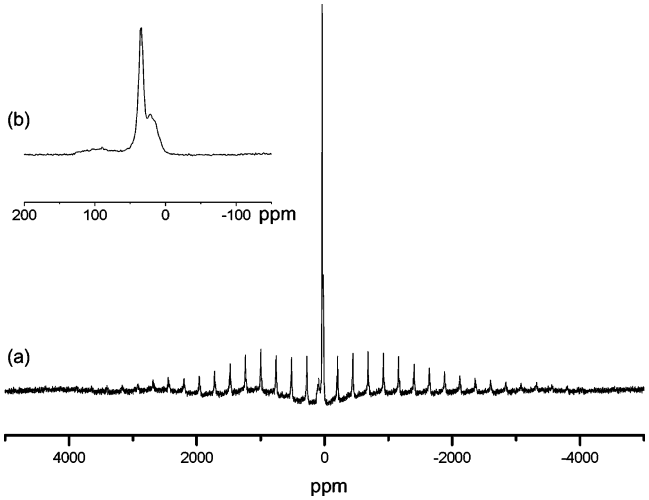

Figure 8. ^{45}Sc one-pulse MAS NMR spectrum of compound **1**. Spinning speed: 35 kHz. (a) whole spectrum, (b) enlargement of the central transition. Recycle delay: 4 s.

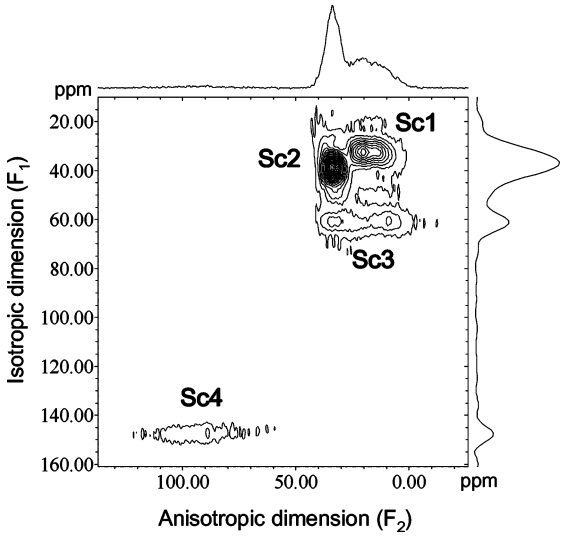

Figure 9. ^{45}Sc 3QMAS NMR spectrum of compound **1**. Spinning speed: 35 kHz. Recycle delay: 4 s.

and F2 sites ($\omega_1 + \omega_2$) and the two values of ω_A are those for the F1 and F2 sites, the DQ MAS NMR spectrum is in complete agreement with the crystallography and shows that the F1 and F2 sites are close to each other, an F1 site is far from another F1, and F2 is far from another F2 (Figure 4).

The sidebands in the ^{45}Sc one-pulse MAS spectrum (Figure 8) spread over a large frequency range of about 1.2 MHz (~8000 ppm). There are two broad resonances at 20 and 90 ppm and a sharp resonance at 34 ppm. A ^{45}Sc multiple quantum MAS (MQMAS) experiment was performed to resolve the four different scandium sites (Figure 9). The resonance at around 90 ppm is extremely broad and can be assigned to a Sc site in distorted local environment. According to the ranges of bond angles and bond lengths calculated from crystallographic data, it can be assigned to Sc4, ScO_6 site (Figure 10). The sharp resonance at 34 ppm is associated with a small second-order quadrupolar broadening in the anisotropic dimension, and hence it can be assigned to the least distorted Sc site, Sc2 (ScO_4F_2). On the basis of the O(F)−Sc−O bond angle distributions, the resonances at around 33 and 63 ppm in isotropic dimension are then

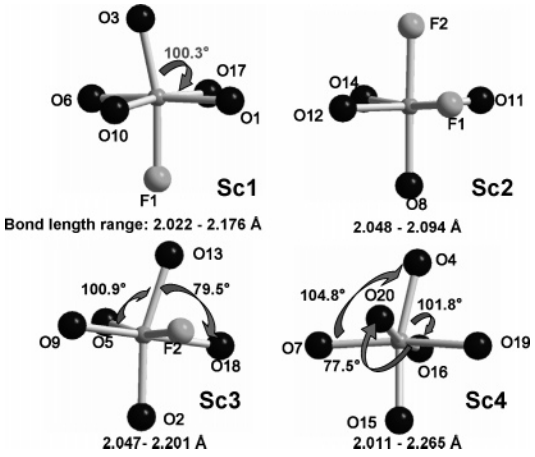

Figure 10. Bonding environment around each Sc atom

Table 4. ^{45}Sc Quadrupolar Parameters of Compound 1

Sc site	δ_{iso}/ppm	C_Q/MHz	η_Q
Sc1	25	8.2	0.2
Sc2	34	<1[a]	[a]
Sc3	46	14.6	0.2
Sc4	127	15.0	0.6

[a] Quadrupolar line shapes not clear enough to extract the parameters.

assigned to the Sc1 site and Sc3 sites, which are located in more and less symmetric environments, respectively. The quadrupolar parameters of the four scandium sites have been extracted from the slices from the 3QMAS spectrum (Table 4). The results show that ^{45}Sc NMR is a very sensitive tool in detecting scandium local environment. The quadrupolar parameters for Sc4 site are very similar to the quadrupolar parameters previous reported for Sc_2O_3.[9]

^{45}Sc/^{19}F REDOR NMR experiments were performed to study the proximity between scandium and fluorine and to confirm the assignments. The REDOR difference spectrum shows the only resonances from the scandium sites which are close to fluorine (Figure 11). The ^{45}Sc

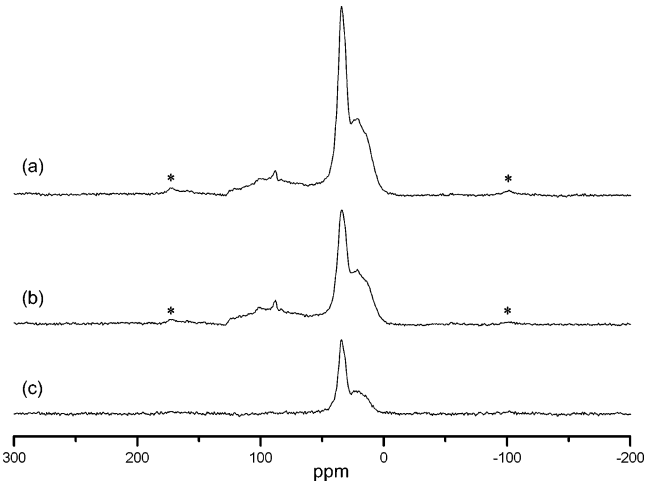

Figure 11. ^{45}Sc/^{19}F REDOR NMR spectra of compound **1**. Spinning speed: 20 kHz. A total dephasing time of 0.5 ms (corresponding to 10 rotor cycles) was used. (a) Spectrum of control experiment without irradiation on ^{19}F channel, (b) spectrum of double resonance experiment with irradiation on ^{19}F channel, (c) difference spectrum obtained by subtracting the spectrum in b from that in a. Recycle delay: 4 s. Asterisks denote spinning sidebands.

resonance at 90 ppm cannot be seen from the difference spectrum, which confirms that this resonance is due to the Sc4 site, because this is the only Sc site that is not directly bonded to fluorine. The largest drop in intensity, between the control (a) and double resonance (b) experiments, is seen for the sharp resonance at 34 ppm (and numbers), which again suggests this resonance is due to the Sc2 site, because Sc2 is the only scandium site near both fluorine sites.

Conclusion

This work describes new three-dimensional scandium and indium fluorophosphate frameworks $(C_6H_{14}N_2)$-$M_4F_2(PO_4)_4 \cdot 4H_2O$ (M = Sc, In), which have been synthesized under hydrothermal conditions using DABCO as a structure-directing agent. Their structure features an inorganic framework built of MO_5F, MO_4F_2, $MO_4(OH_2)_2$ octahedra, and PO_4 tetrahedra. As all the P−O bonds are further linked to M by corner-sharing, these structures suggest the possibility of forming more complete metal phosphate frameworks without any dangling M−O or P−O bonds. These complete frameworks should be more thermally stable thus more readily applicable to various areas common in microporous materials such as catalysis and ion-exchange. The structure of the Sc-compound was further characterized by solid-state NMR spectroscopy. The environment around Sc, P, and F were carefully examined. All the NMR results are consistent with the crystallographic findings. In particular, ^{45}Sc NMR was a great tool to observe the local environment of Sc atoms.

Acknowledgment. This work was supported by the National Science Foundation through a grant to J. B. Parise (DMR-0137780). H. Park thanks the Natural Science and Engineering Council of Canada for PGS-B scholarship. L. Peng thanks Dr. Martine Ziliox at Center for Structural Biology, SUNY at Stony Brook for the help in obtaining high-field (14.1 T) NMR data, Dr. K. Eichele for providing WSolids NMR simulation package, and Center for Environmental Molecular Sciences (CEMS) at Stony Brook for financial support.

Supporting Information Available: The pulse sequences and the coherence pathways of NMR on compound **1** and the X-ray structural information on compounds **1** and **2**. X-ray crystallographic files. This material is available free of charge via the Internet at http:// pubs.acs.org.

CM048764R